



# 17

## Modelling Tidal River Salinity in Coastal Bangladesh

Lucy Bricheno and Judith Wolf

### 17.1 Introduction

In the Ganges-Brahmaputra-Meghna (GBM) delta, river water is widely used to irrigate crops. In recent years there has been an increase in river salinity (Dasgupta et al. 2014). This can affect soil salinity by inundation (if no defences or polders are breached) or by seepage through embankments which has led to an increase in soil salinities, particularly in the west, close to the Sundarbans forest region. This change has potential consequences for land use practices and livelihoods for the delta population. For example, some landowners and farmers have already chosen to convert freshwater rice paddies to brackish water shrimp farms, which may take decades to reverse. Understanding how changing climate (changes in the monsoon rains, leading to changing freshwater flow) may affect future salinity levels is therefore an important topic. In this research, the Finite Volume Coastal Ocean Model (FVCOM)

---

L. Bricheno (✉) • J. Wolf  
National Oceanographic Centre, Liverpool, UK

model has been used to make future projections of river salinity which are used in the assessment of future soil salinity and agricultural productivity (see Chaps. 18 and 24).

## 17.2 The Ganges-Brahmaputra-Meghna (GBM) Delta

With an average freshwater discharge of around 40,000 m<sup>3</sup>/s/year, the GBM river system has the third largest discharge worldwide. The GBM river delta is a low-lying fertile area covering over 100,000 km<sup>2</sup> in India and Bangladesh and is thus classified as a megadelta (Woodroffe et al. 2006). This large discharge forms a large offshore freshwater plume, and the freshwater signal can be observed far offshore, for example, consider World Ocean Atlas/observations from the Soil Moisture and Ocean Salinity (SMOS) satellite in Fig. 17.1. The GBM delta is generally migrating eastwards, and the majority of the freshwater is channelled through the Padma (or Lower Meghna) River (Brammer 2014). There is some limited discharge in the western estuarine section, with the only source of freshwater, the Gorai River. There are some defunct river channels behaving as tidal creeks, but not as sources of freshwater.

Northern Bay of Bengal is mesotidal, with tidal ranges at the coast, varying from two metres to over four metres. Large tides at the coast can penetrate far inland, with tidal variability being observed as far as 200 km

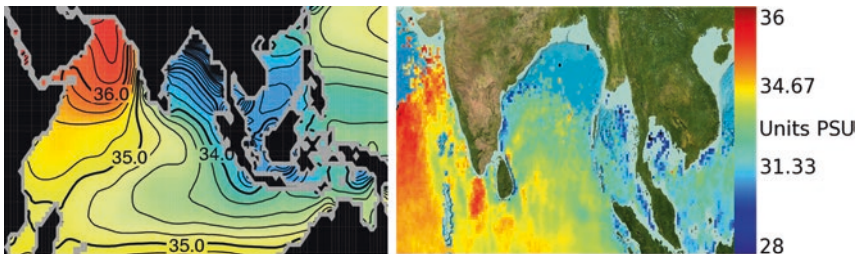


**Fig. 17.1** Annual average sea surface salinity from World Ocean Atlas (left) and SMOS (right) (Reproduced with permission from Antonov et al. 2010, and data from BEC 2010, respectively)

from the coast. Water levels in the delta are also significantly affected by the large volume of river discharge, which can raise mean water depths by as much as four metres.

### 17.3 River Salinity Within the Delta

Salinity is defined as the salt concentration (e.g. sodium and chloride) in water. It is measured in unit of PSU (practical salinity unit<sup>1</sup>). The averaged salinity in the global ocean is 35.5 PSU, while freshwater (e.g. inland lakes or rivers) has salinity close to 0 PSU. Observations of river salinity in Bangladesh and the study area are limited. There are a few point samples of electrical conductivity available, often only during the dry season when salinities are high. Even with this limited data, a clear spatial pattern emerges; Dasgupta et al. (2014) present a contour map, showing a strong longitudinal gradient, with the highest salinities (30+ PSU) in the west of the GBM delta and fresher river waters (<5 PSU) in the east. There are also higher salinities around the coast of around 10 PSU in places. However, this broad pattern does not capture the complex pattern of river salinity in the delta system.

To help address this and provide calibration for the high resolution model FVCOM (Chen et al. 2003), a field survey of salinity levels and river soundings was carried out (see Jahan et al. 2015, data available on request). Using this data the spatial variability of salinity of and changing river salinity over a tidal and seasonal cycle for the delta can be simulated. River cross-section soundings are also primary input to any river/estuary hydraulic/hydrodynamic model. As for most developing countries, there is a lack of sufficient bathymetric data in Bangladesh. The bathymetry of the whole Sundarbans area has never been measured fully, so a bathymetric survey was commissioned. The location of historic (prior to this research) and new survey cross-sections is shown in Fig. 17.2. Besides taking sections, the surveyors also collected soil and water samples and point soundings along the length of the Ganges River.

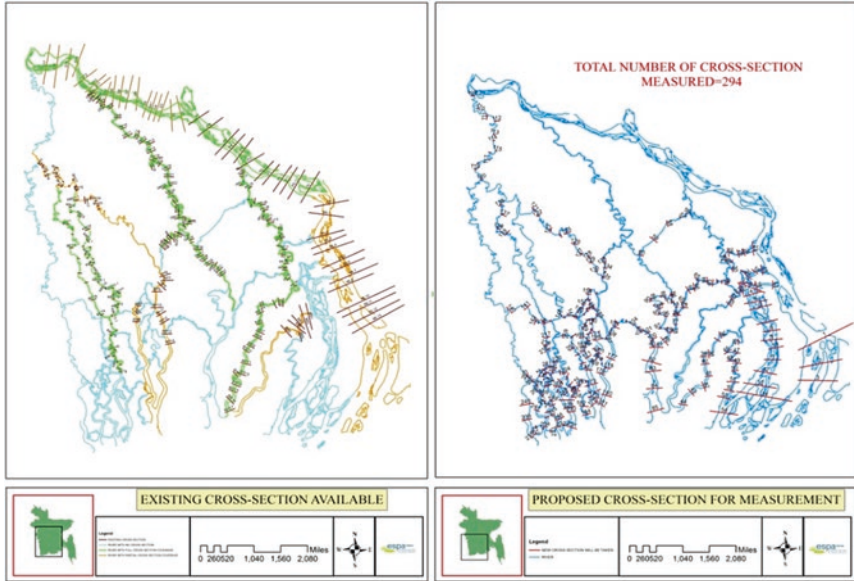


**Fig. 17.2** Mean high water salinity observed during March to May 2014 (left). Modelled mean surface salinity during March to May 2000 (right). Both colour scales show salinity between 0 and 35 PSU

## 17.4 FVCOM Model

The FVCOM model is an unstructured finite volume, 3D baroclinic model which was developed for use in estuarine systems and has since been applied to wider areas (Chen et al. 2006). It can model the effects of tides, freshwater flow, saline water intrusion and sea-level rise. At the Bay of Bengal open boundary, the model is forced by hourly ocean tidal data and daily temperature and salinity from the Bay of Bengal Global Coastal Ocean Modelling System (GCOMS) model (see Chap. 14 and Kay et al. 2015). Figure 17.3 shows the observed river salinity data compared with a FVCOM simulation for 2000. The observations are single snapshots in time, while the modelled results represent the modelled mean for three months. The spatial distribution of the observed salinity is well captured in the model. The modelled salinity is slightly high in the far western section (around the Sundarbans) while salinities are under-predicted (i.e. too fresh

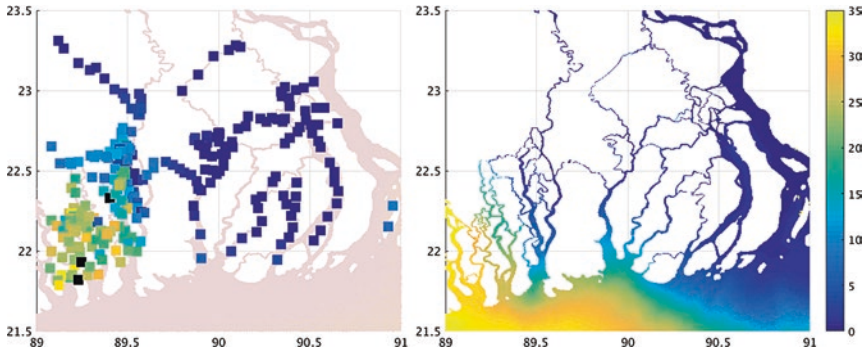


**Fig. 17.3** Locations of river cross-sections: existing sections (left), newly surveyed sections (right) (Reproduced under Creative Commons Attribution 4.0 International License from Bricheno et al. 2016)

in the model) in the Balaswar river (centred at 89.5 East). This disparity between the model and observations may be due to problems in channel connectivity—where freshwaters are unable to penetrate far enough to the west due to small river channels missing in the model. Overall the root mean square error with respect to observations is 5.5 PSU. Even though a direct comparison is not possible, the two results are correlated with an R-squared value of 0.69 (where 0 is uncorrelated, and 1 is perfectly correlated).

Figure 17.4 shows the final model bathymetry developed for this research. It extends inland to the tidal limit and the confluence of the Ganges, Meghna and Brahmaputra, avoiding the need for a separate river model to introduce the freshwater flow. The model is run with 11 vertical levels and variable horizontal resolution between 10 km (at the open boundary) and 50 m, within narrow river channels. The challenge in constructing this model grid was to generate a good-quality mesh and bathymetry which allows the model to produce accurate flows through the delta region. The observations of tidal level within the delta are used to validate the basic hydrodynamics (Bricheno et al. 2016). The modelled sea surface elevations have been compared against tidal data and water level observations inland. At the open coast, where tides are dominant, the model performs well, giving confidence in its abilities. FVCOM was able to accurately model the tidal ranges in the central delta; however

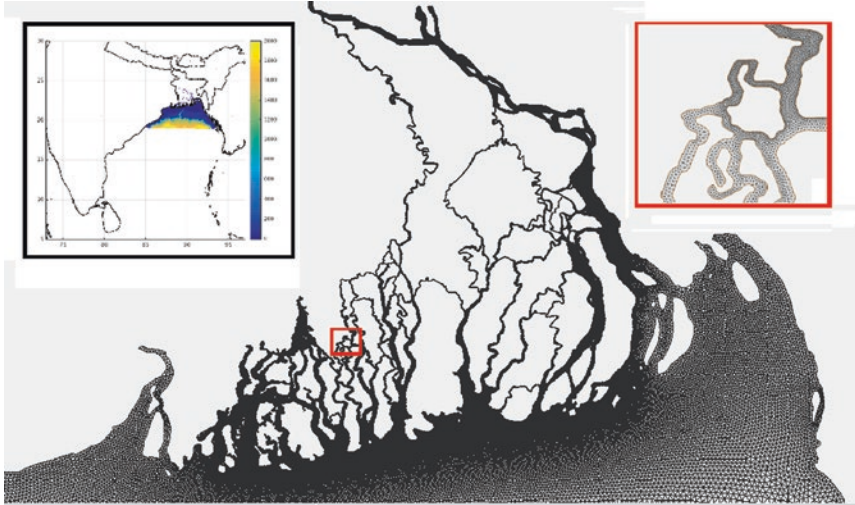


**Fig. 17.4** Unstructured model grid location within the Bay of Bengal (left inset map) and close-up of Sundarbans channels (right inset)

there was some under-prediction of the tidal range in the Sundarbans forest region, and within the Lower Meghna.

River discharge is applied as an upstream boundary; a volume of freshwater is introduced to the model at a single grid point at the northern boundary of the model (indicated in Fig. 17.5). The daily discharge volume rate comes from the hydrological INCA model (see Chap. 13 and Whitehead et al. 2015).

Following the model validation, FVCOM is then run for discrete future time slices (described in Table 17.1) to examine projected changes in tidal range and river salinity. Meteorological forcing is not applied locally in the delta model, but the input to INCA comes from the Regional Climate Model (Chap. 11 and Caesar et al. 2015). The model runs are therefore consistent with the scenarios of changing sea level and freshwater flow used elsewhere in the research.

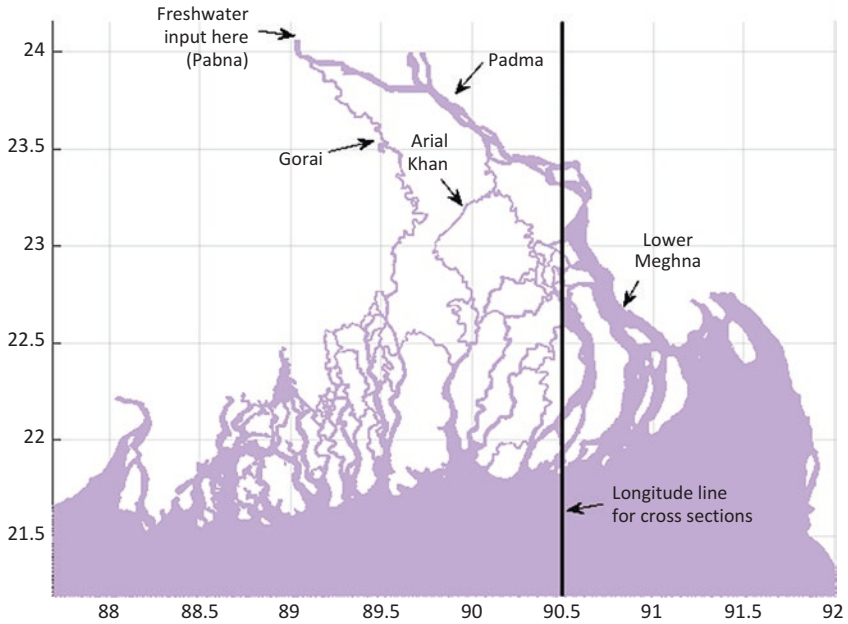


**Fig. 17.5** Map showing river channel names, freshwater input location and section line discussed in the text

**Table 17.1** Summary of scenario runs with annual river discharge over time discussed in this chapter

Scenario	Description	Climate and management	MSLR (cm)	Year	Annual river discharge (m <sup>3</sup> )	'Wet' or 'dry'
1	Baseline	Q0+business as usual	0.0	2000–2001	9,928,407	
2	Mid-century	Q0+business as usual	31.96	2047–2048	13,979,424	Wet
3	Mid-century	Q8+less sustainable	27.06	2050–2051	10,011,085	Dry
4	End century	Q8+more sustainable	58.77	2082–2083	16,517,208	Wet
5	End century	Q0+business as usual	59.01	2097–2098	10,978,254	Dry

## 17.5 Baseline River Salinity Modelling

Water levels in the delta are controlled by a balance between river and tidal flow, acting on different timescales. Throughout the year the situation can change, from tides controlling the water levels in the dry season to dominance by river flow during the monsoon. Some sensitivity to model bottom roughness is seen in the simulations, though the magnitude of these changes is small in the context of tidal range and seasonal water level changes associated with freshwater.

Figure 17.6 shows modelled surface salinity from the baseline simulation described in Table 17.1. As there is a continuous data set from the model, the mean and maximum are calculated from the full annual data set, while Fig. 17.2 compares point observations with a modelled map for the March to May period.

It may be seen that the salinity is higher in the west of the study region around the Sundarbans forest. This is because the majority of freshwater discharges occur through the eastern distributaries, especially the Meghna Estuary, and the western delta is composed mainly of tidal creeks with little or no freshwater input. In the FVCOM delta model, there is only one point of freshwater input (marked on Fig. 17.5). The network of river distributaries then carries this to the Bay of Bengal. The model may be missing additional freshwater inputs from smaller distributaries and Indian rivers that enter the

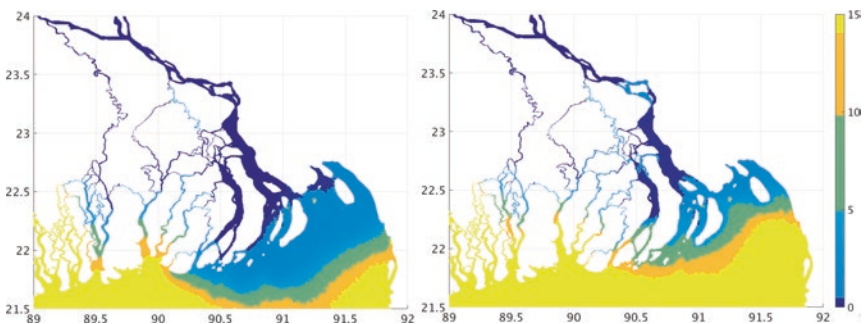


**Fig. 17.6** Mean high water salinity during 2000 (left) and maximum high water salinity during 2000 (PSU) (right)



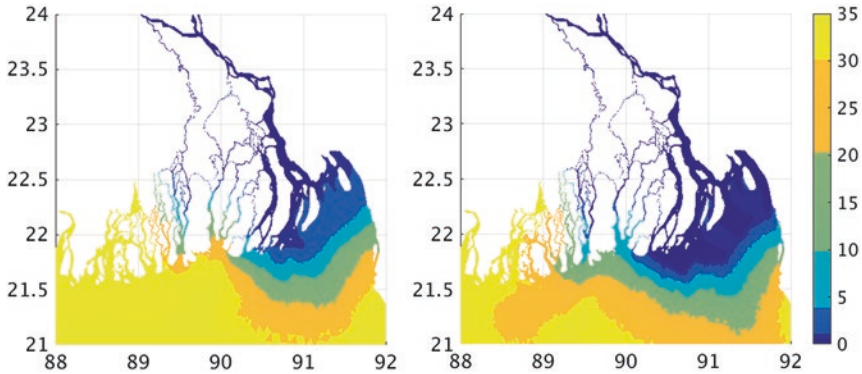


**Fig. 17.7** Spring (March–April–May) mean salinity (left) and autumn (September–October–November) mean salinity (right) during 2000 (PSU)

west of the delta. Freshwater input to the model is also limited, as surface precipitation and evaporation are not included.

Figure 17.7 shows how seasonal discharge associated with monsoon rains alters river surface salinity in the delta. The spring mean (an average salinity for March, April, May) represents the end of the dry season, when sea water has been able to penetrate further inland, unopposed by river outflow. The second panel shows average salinity for the autumn (September, October, November) after a period of heavy rainfall during the monsoon. At this point in the year, a large volume of river water has been discharged through the delta, creating a freshwater plume offshore. Though the large channels of the lower Meghna remain relatively fresh throughout the year, the salinity in the narrow channels in the central and western sectors of the delta are more strongly affected by these seasonal fluctuations.

Another controlling factor on river salinity is the effect of tidal mixing. Figure 17.8 shows how the freshwater plume moves in and out over the course of a 12.4 hour cycle. The largest differences are seen along the sharp front, where fresh river waters of  $<3$  PSU meet ocean waters of  $>30$  PSU. Further inland the impact of the tide is also observed: leading to differences in salinity of 3 PSU and above.

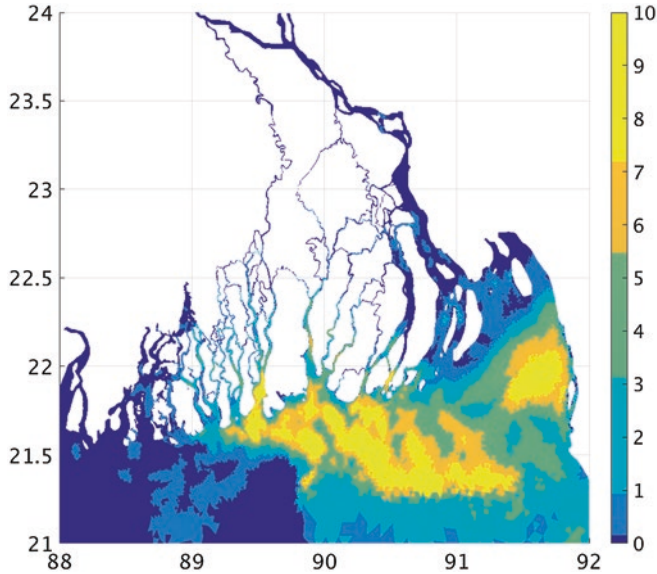


**Fig. 17.8** Map showing the change in salinity (PSU) comparing daily high water and low water salinity for a 25 hour period on a spring tide during the dry season

These processes operate on very different timescales: day-to-day, the tides dominate while the annual river discharge cycle controls local salinity on a longer annual scale.

### 17.5.1 The Freshwater Plume

Further offshore, away from the narrow river channels, freshwater enters the Bay of Bengal and spreads out into a coastal plume. Figure 17.9 shows the extent of the freshwater plume offshore and its structure in the vertical during the dry (upper) and wet season (lower). The modelled plume is quite well mixed in the vertical, though some structure of fresher river waters overlying saltier sea water is observed in the July snapshot. When the water column stratifies following the monsoon, the freshwater layer can be between 5 and 10 m thick in the vertical. The extent and position of this freshwater plume may have implications for coastal water quality, nutrient fluxes and fisheries.

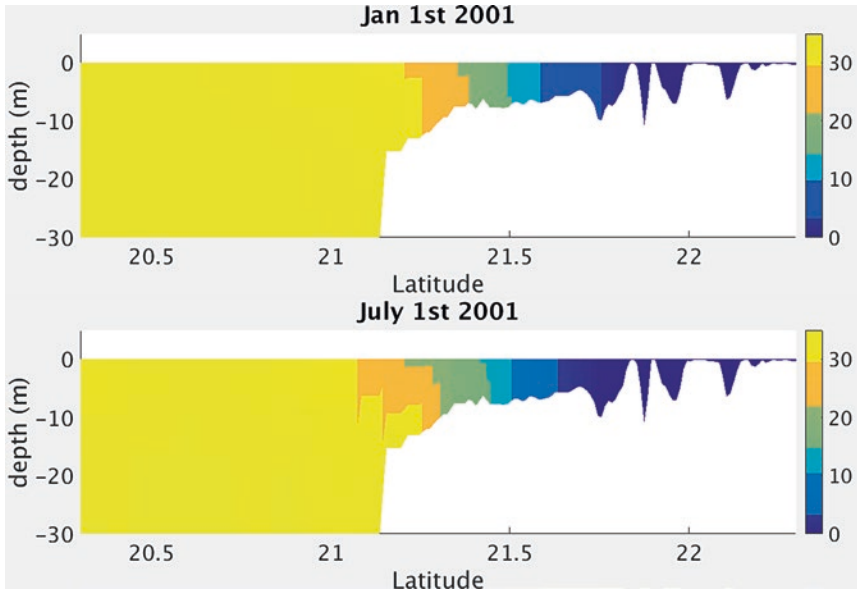


**Fig. 17.9** Vertical profiles of salinity along 90.5E comparing 1 January 2001 (upper) and 1 July 2001 (lower)

### 17.5.2 Salinity Projections

In order to investigate potential future river salinities, five scenarios were run: one as a historic baseline and four futures (Table 17.1). The future scenarios were designed based on the discharge rates provided by the INCA model to encapsulate the full range of possible climate states and wet/dry years. Cumulative river discharge was therefore used to guide the selection of scenario years; for a mid-century period (2030–2059) and a late-century period (2070–2099), all river discharge years were examined, and those with maximum/minimum cumulative annual discharge were selected to be simulated in FVCOM. The annual cumulative discharge volume for each scenario year is shown in Fig. 17.10. A rate of changing sea-level rise consistent with the discharge year was applied at the open ocean boundary. Mean sea-level rise (MSLR), as described in Chap. 14 and Kay et al. (2015), was applied. The total MSLR for each year is shown in Table 17.1

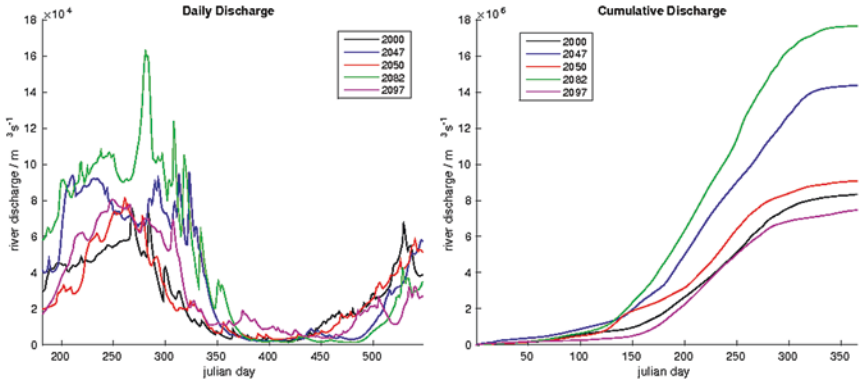


**Fig. 17.10** Daily river discharge used as model forcing (left) and cumulative annual discharge (right) in  $\text{m}^3$  for five scenario years. The scenarios are run from monsoon to monsoon period, starting on 1 June each year

In addition to changes in total river volume discharged during the year, it is also important to consider the nature of freshwater input and tidal influence. The timing and intensity of freshwater input is closely related to the intensity of the monsoon as illustrated by the left hand panel of Fig. 17.10 which shows the daily river discharge entering the model at a site close to the city of Pabna, situated on the Padma (Ganges) River. In ‘wet’ years (blue and green curves) there is an early and sharp monsoon onset around the middle of July (day 200). A more gradual and later onset (around day 220—early August) occurs during the two ‘dry years’ (pink and red curves). The future tidal range is projected to become larger, although not in a spatially homogenous fashion. Combined with an increase in mean sea level, this leads to an increase of salt intrusion into the delta (e.g. see Fig. 17.11).

The spatial structure of the front is complex and ‘pulses’ in and out on a tidal time scale of 12.4 hours. There is also considerable vertical structure in the profile of salinity, with a fresher layer overlying salty waters. Tides advect salt water in and out, but also contribute to mixing in the vertical.

Figure 17.12 shows the distribution of mean and maximum annual salinity in the study area under the baseline scenario. A strong east-west profile is observed, with freshwaters in the eastern section, dominated by

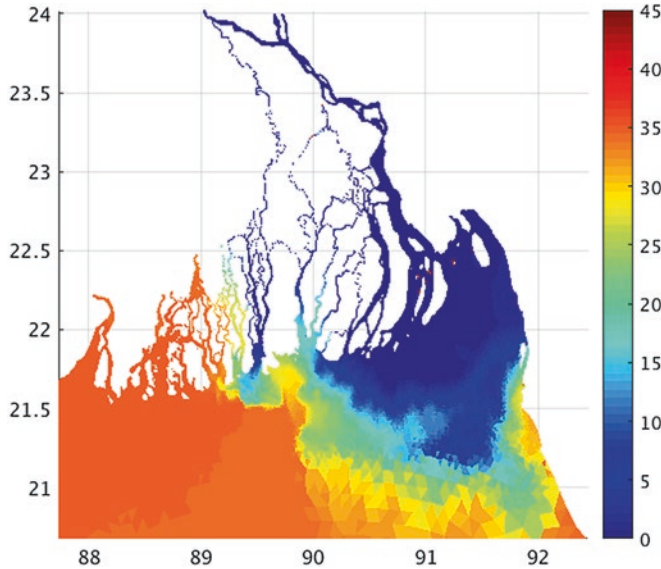


**Fig. 17.11** Snapshot of surface salinity (PSU) during the wet season under scenario 5 (July 2098)

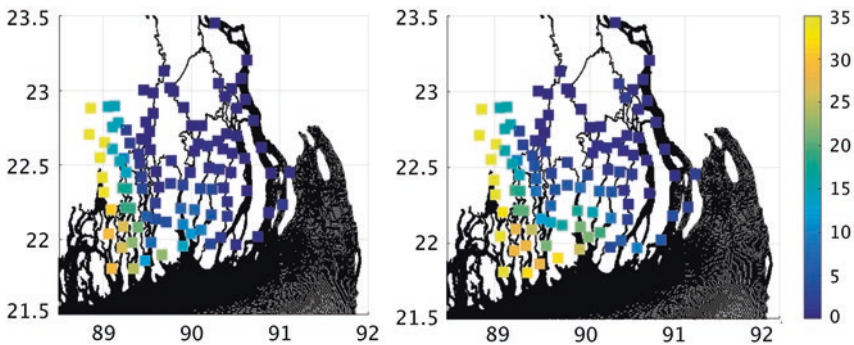


**Fig. 17.12** Mean (left) and maximum (right) salinity during the baseline simulation 2000–2001 (Scenario 1 in Table 17.1)

outfall from the Meghna. The drier western section is saltier overall, with maximum values approaching those of seawater. There may be some over-prediction of salinity in the very west of the model, due to the limited input of freshwater in this area.

**Table 17.2** Ocean salinity forcing levels used for modelled scenarios

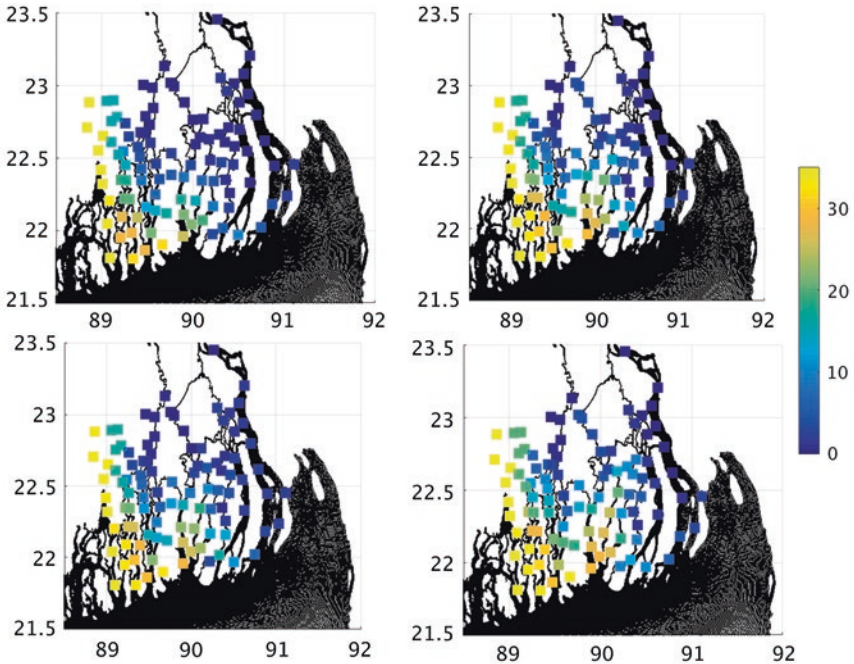
Scenario years	2000–2001	2047–2048	2050–2051	2082–2083	2097–2089
Mean 'ocean' salinity (PSU)	34.39	34.10	34.38	33.99	34.22

Table 17.1 shows that the annual discharge in scenarios 1 and 5 are similar. However, surface salinity is relatively high across much of the delta. This may be due to a change in ocean conditions which are represented by salinity evolution at the open boundary of the model. Table 17.2 shows the mean salinity in the forcing model GCOMS at 19°N, which is used to drive the FVCOM model.

The numbers in Table 17.2 indicate that mean ocean salinities do not vary greatly over time. This suggests that the rise observed in river salinity may therefore be largely related to hydrodynamics, higher mean sea levels and changes in tidal conditions allowing ocean water to penetrate further inland. This is shown most clearly in the west of the study area, where the largest increases in salinity levels along the rivers are projected. In the east of the study area (e.g. at the mouth of the Meghna River), this potential increase is offset due to additional freshwater discharge meaning salinity levels remain relatively unchanged over time.

The maximum annual salinities for four future scenarios within the delta are shown in Fig. 17.13. The top row (mid-century) simulations see higher maximum values in the Western Estuarine System when compared with the baseline year, while the eastern estuary remains largely unchanged.

In the far future simulations (bottom row), the effect of salt intrusion is seen more strongly, particularly in the 'dry' year scenario (5—low freshwater input and no change in management). Under this scenario, high values exceeding 15 PSU are observed throughout the central estuarine section, and salinities exceeding 5 PSU are seen at the mouth of Lower Meghna.



**Fig. 17.13** Annual maximum salinities for 103 selected points under the four future scenarios described in Table 17.1. Clockwise from top left: S1, S2, S4, S3

## 17.6 Conclusion

River salinity in the GBM delta can be simulated with a variable resolution hydrodynamic model. Salt intrusion has a pronounced spatial pattern, with the saltiest river waters observed in the western estuarine section and the Sundarbans forest. Waters become progressively fresher moving towards the east and the mouth of the Lower Meghna. There is a strong seasonal signal in the freshwater distribution controlled by variable river discharge from the monsoon to the dry season including within the freshwater plume which alters size, position and vertical structure throughout the year.

Tidal excursion of the freshwater front can alter local river salinity by between two and five PSU over the course of a day. River salinity is largely controlled by a combination of annual monsoon discharge and tidal processes. In the western and central estuarine sections salt intrusion at the coast is the dominant factor. In the eastern section, the increased river flow and increased sea level are more balanced, so there is little future change in salinity in the mouth of the Meghna.

Under all future projections of freshwater input and ocean changes, salinity is predicted to increase in the river channels. This increase is more pronounced in the central and western estuarine section with implications for agriculture, shrimp farming and local well-being (see Chaps. 21, 24 and 27).

## Note

1. A unit based on the properties of seawater conductivity. It is equivalent to parts per thousand or grams per kilogramme. The highest observed salinities (more than 40 PSU) are found in the Dead Sea.

## References

- Antonov, J.I., D. Seidov, T.P. Boyer, R.A. Locarnini, A.V. Mishonov, H.E. Garcia, O.K. Baranova, M.M. Zweng, and D.R. Johnson. 2010. Volume 2: Salinity. In *World Ocean Atlas 2009; NOAA Atlas NESDIS 69*, ed. S. Levitus, vol. 184. Washington, DC: U.S. Government Printing Office.
- BEC. 2010. *Sea surface salinity data*. <http://bec.icm.csic.es/>. Accessed 14 June 2017.
- Brammer, H. 2014. Bangladesh's dynamic coastal regions and sea-level rise. *Climate Risk Management* 1: 51–62. <https://doi.org/10.1016/j.crm.2013.10.001>.
- Bricheno, L.M., J. Wolf, and S. Islam. 2016. Tidal intrusion within a mega delta: An unstructured grid modelling approach. *Estuarine Coastal and Shelf Science* 182: 12–26. <https://doi.org/10.1016/j.ecss.2016.09.014>.
- Caesar, J., T. Janes, A. Lindsay, and B. Bhaskaran. 2015. Temperature and precipitation projections over Bangladesh and the upstream Ganges, Brahmaputra



- and Meghna systems. *Environmental Science-Processes and Impacts* 17 (6): 1047–1056. <https://doi.org/10.1039/c4em00650j>.
- Chen, C.S., H.D. Liu, and R.C. Beardsley. 2003. An unstructured grid, finite-volume, three-dimensional, primitive equations ocean model: Application to coastal ocean and estuaries. *Journal of Atmospheric and Oceanic Technology* 20 (1): 159–186. [https://doi.org/10.1175/1520-0426\(2003\)020<0159:augfvt>2.0.co;2](https://doi.org/10.1175/1520-0426(2003)020<0159:augfvt>2.0.co;2).
- Chen, C., R.C. Beardsley, and G. Cowles. 2006. *An unstructured grid, finite-volume coastal ocean model. FVCOM user manual*. 2nd ed. Cambridge, MA: School of Marine Science and Technology at the University of Massachusetts-Dartmouth (SMAST/UMASSD).
- Dasgupta, S., F.A. Kamal, Z.H. Khan, S. Choudhury, and A. Nishat. 2014. *River salinity and climate change: Evidence from coastal Bangladesh*. Policy working paper series 6817. Washington, DC: The World Bank. <http://documents.worldbank.org/curated/en/522091468209055387/River-salinity-and-climate-change-evidence-from-coastal-Bangladesh>. Accessed 11 Apr 2014.
- Jahan, M., M.M.A. Chowdhury, S. Shampa, M.M. Rahman, and M.A. Hossain. 2015. *Spatial variation of sediment and some nutrient elements in GBM delta estuaries: A preliminary assessment*. Proceedings of the International Conference on Recent Innovation in Civil Engineering for Sustainable Development (IICSD-2015), December 11–13, Dhaka University of Engineering and Technology, Gazipur.
- Kay, S., J. Caesar, J. Wolf, L. Bricheno, R.J. Nicholls, A.K.M.S. Islam, A. Haque, A. Pardaens, and J.A. Lowe. 2015. Modelling the increased frequency of extreme sea levels in the Ganges-Brahmaputra-Meghna delta due to sea level rise and other effects of climate change. *Environmental Science-Processes and Impacts* 17 (7): 1311–1322. <https://doi.org/10.1039/c4em00683f>.
- Whitehead, P.G., E. Barbour, M.N. Futter, S. Sarkar, H. Rodda, J. Caesar, D. Butterfield, L. Jin, R. Sinha, R. Nicholls, and M. Salehin. 2015. Impacts of climate change and socio-economic scenarios on flow and water quality of the Ganges, Brahmaputra and Meghna (GBM) river systems: Low flow and flood statistics. *Environmental Science-Processes and Impacts* 17 (6): 1057–1069. <https://doi.org/10.1039/c4em00619d>.
- Woodroffe, C.N., R.J. Nicholls, Y. Saito, Z. Chen, and S.L. Goodbred. 2006. Landscape variability and the response of Asian megadeltas to environmental change. In *Global change and integrated coastal management: The Asia-Pacific region*, ed. N. Harvey, 277–314. Dordrecht: Springer.

**Open Access** This chapter is licensed under the terms of the Creative Commons Attribution 4.0 International License (<http://creativecommons.org/licenses/by/4.0/>), which permits use, sharing, adaptation, distribution and reproduction in any medium or format, as long as you give appropriate credit to the original author(s) and the source, provide a link to the Creative Commons license and indicate if changes were made.

The images or other third party material in this chapter are included in the chapter's Creative Commons license, unless indicated otherwise in a credit line to the material. If material is not included in the chapter's Creative Commons license and your intended use is not permitted by statutory regulation or exceeds the permitted use, you will need to obtain permission directly from the copyright holder.

